



TESIS DOCTORAL

Optimización de reactores fotocatalíticos para el tratamiento de aguas: fuente de iluminación, configuración y tipo de catalizador

Autor:

Miguel Martín Sómer

Directores:

Javier Marugán Aguado

Rafael van Grieken Salvador

Programa de Doctorado en Tecnologías Industriales:
Química, Ambiental, Energética, Electrónica, Mecánica y de
los Materiales

Escuela Internacional de Doctorado

2019

Summary

I. INTRODUCTION.

Nowadays, the protection of the environment stands out as one of the main problems of modern societies with great social, political, technological and economic repercussion. The growth of the population and the expansion of numerous agricultural and industrial activities have led to the necessity of implementing a strict environmental legislation that regulates the quality of the main effluents generated for its discharge in municipal collectors or directly to the environment. Water availability is increasingly scarce, and insufficient natural water resources in arid and semi-arid zones constitute a serious problem for the population settled in them. In European countries, 54% of total water consumption is for industrial use, according to the UNESCO report "Water for all, Water for life"¹. Part of the water is discharged after being used, containing waste resulting from the production process. Therefore, industrial wastewater has particular characteristics depending on its origin, which determines its treatment before being discharged into the natural environment. Contamination of surface waters with chemical agents represents a threat to the aquatic environment since, in some cases, this type of contamination has effects such as acute and chronic toxicity to aquatic organisms, accumulation in the ecosystem and loss of habitats and biodiversity, as well as damage to human health. This fact has led to the development of an increasingly restrictive legislation on water quality with the ultimate goal of achieving a good ecological status and sustainable use of European waters. One of the most recent directives developed by the European Parliament and the Council of the European

¹ UNESCO, 'Agua para todos, Agua para la vida', 2003.

Union is Directive 2008/105/EC² concerning water quality standards. According to this Directive, specific measures should be taken against water pollution caused by certain pollutants or groups of these that represent a significant risk to the aquatic environment.

Among the priority research lines of the main organizations for the protection of environment and public health are the so-called contaminants of emerging concern (CECs). This group of pollutants are defined as contaminants previously unknown or not recognized as pollutants whose presence in the environment is not necessarily new but it is new the concern about their possible consequences³. These contaminants are detected at trace level (ng/L) in wastewater and surface water, which confirms that their elimination in conventional water treatment processes is not total. Among the CECs that demand greater and urgent attention can be found: brominated flame retardants, chloroalkanes, pesticides, perfluorinated compounds, drugs and drugs of abuse.

On the other hand, it is important to consider that sustainable water management is not limited only to the non-contamination of water, but also implies enacting savings and efficiency in its use. For this, it is necessary to search for alternative sources of supply, such as the reuse of water. Reclaimed water should be considered as an additional resource that offers both quality and quantity guarantees and that has the possibility of replacing drinking water for uses that require lower quality levels such as

² Unión Europea, 'Directiva 2008/105/CE. Relativa a las normas de calidad ambiental en el ámbito de la política de aguas', *Diario Oficial de La Unión Europea*, 348 (2008), 84–97.

³ L. Damià and M.J. López, 'Contaminación y calidad química del agua: el problema de los contaminantes emergentes', *Instituto de Investigaciones Químicas y Ambientales-CSIC. 2007. Barcelona, 2007*, 1–27.

Summary

irrigation of crops, parks and gardens, cleaning of streets etc. The availability of potable water is a priority objective that is not always easy to ensure, especially in countries such as Spain that suffers from a deficit of water. In addition, the provision of reclaimed water guarantees a non-climate-dependent supply that does not compete with priority uses, guaranteeing supplies for sectors especially sensitive to water deficits such as agriculture or industry. On the other hand, there are also environmental benefits derived from the reuse of water that are especially relevant when the use of a certain volume of reclaimed water replaces the use of a volume from rivers or aquifers⁴.

In Spain, on December 7, 2007, Royal Decree 1620/2007⁵ was approved establishing regulations to be followed regarding the water reuse. This Royal Decree establishes the possible uses of the reclaimed water and the quality necessary for each of them, being one of the main parameters to take into account the microbiological quality.

Advanced oxidation processes have demonstrated their effectiveness in both bacterial inactivation and elimination of persistent contaminants as the CECs. These treatments are based on the generation and use of powerful transient species with high oxidation potentials⁶.

⁴ Ministerio de Medio Ambiente y Medio Rural y Marino, 'Guía para la Aplicación del R.D. 1620/2007 por el que se establece el régimen jurídico de la reutilización de las aguas depuradas', 2010.

⁵ Ministerio de la Presidencia, 'Real Decreto 1620/2007, de 7 de diciembre, por el que se establece el régimen jurídico de la reutilización de las aguas depuradas', *Boletín Oficial Del Estado*, 2007.

⁶ Rachel Fagan and others, 'A review of solar and visible light active TiO₂ photocatalysis for treating bacteria, cyanotoxins and contaminants of emerging concern', *Materials Science in Semiconductor Processing*, 42 (2016), 2–14.

Among the advanced oxidation processes, the photocatalytic processes are of special importance. These processes are based in redox reactions accelerated by the photogeneration of electron-hole pairs of high reducing and oxidizing power respectively. A semiconductor (catalyst) is illuminated with light of energy higher than the band gap (energy difference between the conduction band and the valence band) in the UV-visible range, absorbing the photons and creating the electron-hole pairs. Then, on the one hand, the transfer of electrons by the semiconductor to electron-accepting adsorbed molecules and on the other hand the transfer of electrons from adsorbed electron-donating molecules to the semiconductor takes place. The adsorbed molecules are transformed into ions that subsequently react to achieve the oxidation of the compounds of interest (**figure S.1**). In the case of photocatalytic processes carried out in aqueous solution with semiconductor oxides in the presence of oxygen, it is considered that the holes generated in the semiconductor interact with water molecules generating hydroxyl radicals.

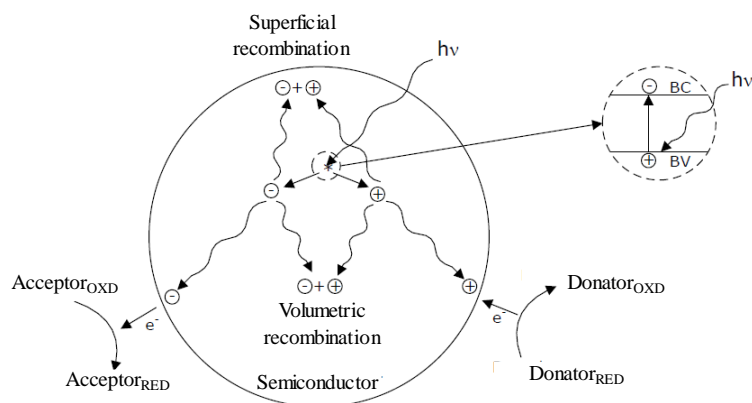


Figure S.1. Diagram of heterogeneous photocatalysis processes⁷.

⁷ Cristina Pablos, 'Desarrollo de procesos fotocatalíticos para la desinfección de agua y aplicación a la regeneración de aguas residuales depuradas', 2013.

Summary

The most commonly used photocatalyst is the commercial material Evonik P25 (before Degussa P25) constituted by a 3:1 ratio between the phases of TiO₂ anatase and rutile⁸. P25 is a stable material, due to its redox potential capable of producing hydroxyl radicals and has the advantages of low toxicity, high active area and low cost.

Due to its absorption spectrum, the activation of TiO₂ requires illumination with wavelengths lower than 400 nm in the UV-A range. Conventional UV lamps, such as low-pressure mercury lamps, have been traditionally used⁹. However, these lamps have low effectiveness in the conversion of electrical energy into light, being the high energy consumption one of the main drawbacks of photocatalytic processes¹⁰. In recent years, LED technology has been developed in the UV range offering numerous advantages over conventional systems such as higher energy efficiency, a longer lifetime, absence of mercury, easily adaptable output or instant on-off¹¹.

⁸ Teruhisa Ohno and others, 'Morphology of a TiO₂ photocatalyst (Degussa, P25) consisting of anatase and rutile crystalline phases', *Journal of Catalysis*, 203.1 (2001), 82–86.

⁹ A. C. Chevremont and others, 'Fate of carbamazepine and anthracene in soils watered with UV-LED treated wastewaters', 2013.

¹⁰ Jyoti P. Ghosh and others, 'A comparison of several nanoscale photocatalysts in the degradation of a common pollutant using LEDs and conventional UV light', *Water Research*, 43.18 (2009), 4499–4506.

Claudio Minero and Davide Vione, 'A quantitative evaluation of the photocatalytic performance of TiO₂ slurries', *Applied Catalysis B: Environmental*, 67.3 (2006), 257–69.

¹¹ Kai Song, Madjid Mohseni, and Fariborz Taghipour, 'Application of ultraviolet light-emitting diodes (UV-LEDs) for water disinfection: A review', *Water Research*, 94 (2016), 341–49.

Mohamed A.S. Ibrahim and others, 'Evaluating the impact of LED bulb development on the economic viability of ultraviolet technology for disinfection', *Environmental Technology*, 35.4 (2014), 400–406.

M. A. Wü Rtele and others, 'Application of GaN-based ultraviolet-C light emitting diodes e UV LEDs e for water disinfection', *Water Research*, 45 (2011), 1481–89.

Moreover, the use of LED makes the design of the reactor significantly more flexible, without being limited by the tubular shape of the mercury lamps. However, the use of LED also introduces important changes in the light distribution achieved along the reactor that must be taken into account. Some studies found in the literature¹² compare the use of LED lighting systems and conventional UV lamps showing no improvements in efficiency when using LED that could be due to an incorrect design of the lighting systems.

In this work, a comparative study between the use of a mercury fluorescent lamp and two LED lighting systems with different light distribution for chemical oxidation and bacterial inactivation has been carried out with the objective of studying the effect of the light distribution inside of the reactor in both the photocatalytic efficiency and the global energy efficiency.

Additionally, another of the main advantages of the development of LED technology is the availability of monochromatic light sources of different wavelengths. The use of wavelengths closer to the visible range has the advantage of showing significantly higher energy efficiencies being an especially attractive option the use of active catalysts in the UV-A/Vis

¹² Jyoti P. Ghosh, Cooper H. Langford, and Gopal Achari, 'Characterization of an LED based photoreactor to degrade 4-chlorophenol in an aqueous medium using coumarin (C-343) sensitized TiO₂', *The Journal of Physical Chemistry A*, 112.41 (2008), 10310–14.

Lanfeng H. Levine and others, 'Feasibility of ultraviolet-light-emitting diodes as an alternative light source for photocatalysis', *Journal of the Air & Waste Management Association*, 61.9 (2011), 932–40.

Seong Hee Kim and others, 'Monitoring of TiO₂-catalytic UV-LED photo-oxidation of cyanide contained in mine wastewater and leachate', *Chemosphere*, 143 (2016), 106–14.

Fatemeh Khodadadian and others, 'Model-Based Optimization of a Photocatalytic Reactor with Light-Emitting Diodes', *Chemical Engineering & Technology*, 39.10 (2016), 1946–54.

Summary

range such iron-based compounds in photo-Fenton processes. In addition, the use of this type of catalysts is interesting not only for the possible energy savings when using artificial light but also for the possibility of using sunlight as a source of illumination.

During the development of this work, the action spectra of P25 and Fe-citrate catalysts at neutral pH has been studied and compared using monochromatic LED sources with emission peaks centered at different wavelengths. Additionally, a semiexperimental calculation of the activity that would be obtained with both catalysts if solar light is used as a source of illumination was carry out and validated.

Another aspect to take into account in photocatalytic processes is the configuration of the catalyst. Generally, it is used in aqueous suspensions, however, it is of special interest carry out the immobilization of the photocatalyst in a substrate in order to avoid the necessity of a subsequent separation step and enabling its recovery and reuse¹³. However, because the immobilization of the photocatalyst results in a reduction of the active surface of the catalyst, loss of photocatalytic activity generally occurs¹⁴. Among the different supports studied in heterogeneous photocatalysis, macroporous reticulated materials such as foams exhibit better mass and

¹³ Javier Marugán, Paul Christensen, and others, 'Synthesis, characterization and activity of photocatalytic sol-gel TiO₂ powders and electrodes', *Applied Catalysis B: Environmental*, 89.1-2 (2009), 273-83.

Beata Tryba, 'Immobilization of TiO₂ and Fe-C-TiO₂ photocatalysts on the cotton material for application in a flow photocatalytic reactor for decomposition of phenol in water', *Journal of Hazardous Materials*, 151.2-3 (2008), 623-27.

Boštjan Erjavec and others, 'Glass fiber-supported TiO₂ photocatalyst: Efficient mineralization and removal of toxicity/estrogenicity of bisphenol A and its analogs', *Applied Catalysis B: Environmental*, 183 (2016), 149-58.

¹⁴ S. Murgolo and others, 'A new supported TiO₂ film deposited on stainless steel for the photocatalytic degradation of contaminants of emerging concern', *Chemical Engineering Journal*, 318 (2017), 103-11.

photon transfer, a large specific surface area and a greater photocatalytic performance than other support materials¹⁵. Therefore, in this work we have studied the immobilization of three different TiO₂ materials in macroporous photocatalytic foams and their performance in the elimination of CECs and water disinfection in both a synthetic water and a real wastewater.

II. MATERIALS AND METHODS.

Photocatalytic systems.

Annular photoreactor.

An annular photoreactor was used to carry out the study of the influence of the light distribution and the influence of the wavelength. The reactor consists of two concentric borosilicate cylindrical tubes with diameters of 3 and 5 cm and 15 cm in length. The reactions were carried out in a closed recirculation circuit with a stirred tank operated by a centrifugal pump with a flow rate of 36 L/min. The total work volume was 1 L. Due to the short residence time and the mixing conditions produced by the reactor inlets it can be assumed that the whole photocatalytic system behaves like a perfect mixing reactor. The illumination source was placed on the axis of the annular section (**figure S.2**), with an irradiated volume of 0.189 L. For the study of the use of the different light sources, a Philips TL 6W black light lamp (Hg-FL) and two LED-based systems with 8 and 40 LEDs were used (LedEngin Model LZ1-00UV00) (**figure S.3**). The LED-based systems

¹⁵ Dong Hao and others, 'Photocatalytic activities of TiO₂ coated on different semiconductive SiC foam supports', *Journal of Materials Science & Technology*, 29.11 (2013), 1074–78

G. Plantard, V. Goetz, and D. Sacco, 'TiO₂-coated foams as a medium for solar catalysis', *Materials Research Bulletin*, 46.2 (2011), 231–34.

Summary

were continuously cooled using a liquid cooling system (Koolance EX2-755). The irradiation of Hg-FL was controlled using opaque neutral filters. In the case of LED systems, the irradiation was controlled through the electric current intensity using the software Eldoled LED driver configuration Toolbox. The distribution of light throughout the reactor with the different illumination sources was calculated using the commercial software Ansys 14.5 (Ansys Inc.[®]).

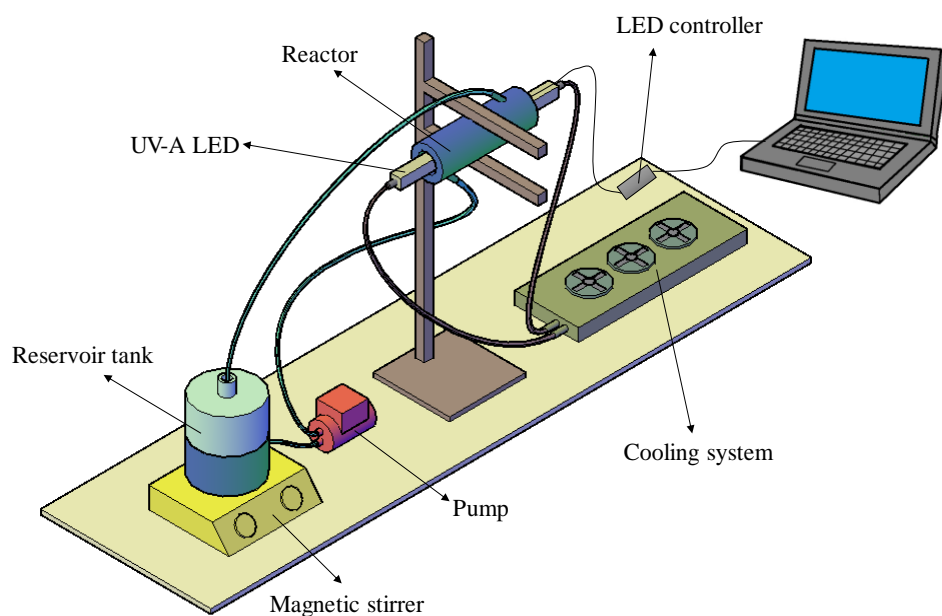


Figure S.2. Schematic representation of the experimental setup of the annular reactor.

For the study of the influence of the wavelength, different systems of 8 LEDs were used with maximum emission peaks centered on 365, 385, 390, 395, 400 and 405 nm. The total irradiation power in each case was

calculated from potassium ferrioxalate actinometry experiments as described elsewhere¹⁶.

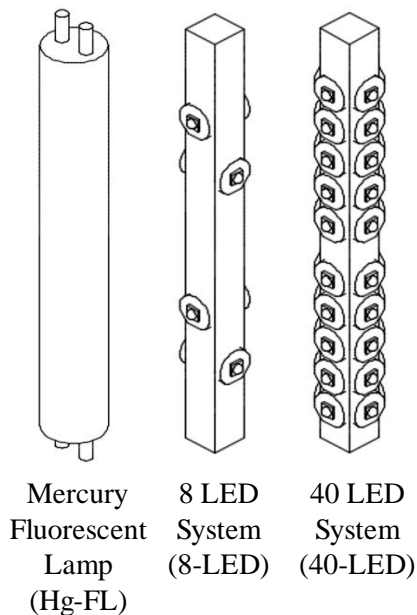


Figure S.3. Schematic representation of the illumination sources.

In the study of the light distribution, commercial P25 in suspension with a fixed concentration of 0.1 g/L was used as a catalyst. In the study of the influence of the wavelength, P25 catalyst and Fe-citrate complex were used with previously optimized concentrations of 0.1 and 0.001 g/L respectively. In the experiments carried out with Fe-citrate catalyst, the concentrations of hydrogen peroxide were set to ensure their non-depletion throughout the reactions.

¹⁶ C. G. Hatchard and C. A. Parker, 'A new sensitive chemical actinometer. II. Potassium ferrioxalate as a standard chemical actinometer', *Proceedings of the Royal Society of London. Series A. Mathematical and Physical Sciences*, 235.1203 (1956), 518 LP-536.

Summary

CPC photoreactor.

To carry out the comparative experiments between the use of P25 and Fe-citrate catalysts under solar irradiation, a CPC reactor was used. The reactor consists of two differentiated circuits in which reactions can be carried out with each catalyst simultaneously. Each circuit has a borosilicate 3.3 Duran® glass tube with an internal diameter of 26 mm and a length of 380 mm located in the focal line of the CPC collector. In each circuit, the fluid is recirculated from a tank using a Model NX-50PX-X centrifugal pump, Pan World Co. Ltd. The total work volume is 1 L with an irradiated volume of 0.2 L. The experiments using this reactor were carried out during July 2017 at the facilities of the Rey Juan Carlos University in Mostoles, Spain (40.33 °N, 3.88 °W). The inclination of CPC reactor was 40 degrees corresponding to the latitude. The irradiance was monitored during the reaction time with a spectrophotometer (Blue Wave, StellarNetInc).

Upflow photoreactor.

For the study of the supported catalyst, a reactor with two differentiated sections was used. A cylindrical region of 15 cm in length, 3 cm of internal diameter and 5 cm of external diameter and a second conical region with a widening of external diameter of 5 to 10 cm (**figure S.4-a**). The illumination source was placed in the axis of the reactor being the total irradiated volume 0.245 L (corresponding to the cylindrical region). The rest of the photocatalytic system was similar to that shown in **figure S.2** being in this case the total work volume 3 L. The lighting source used was the 40 LED source shown in **figure S.3**.

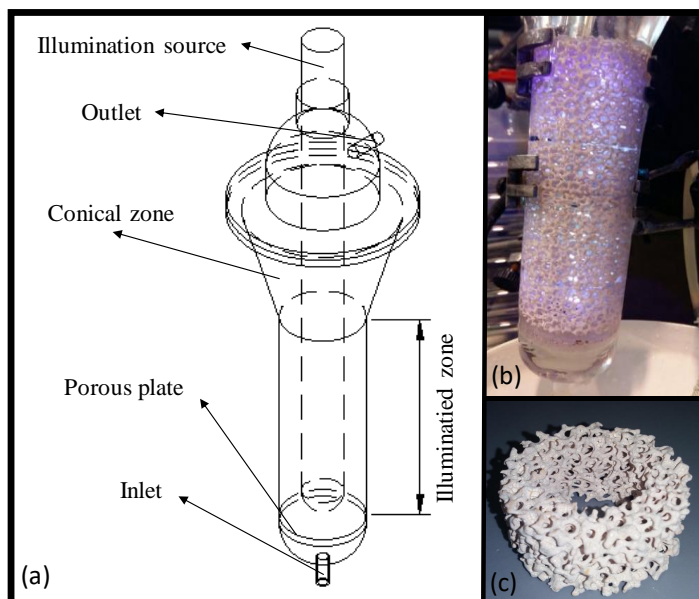


Figure S.4. (a) Schematic representation of the upflow reactor (b) photograph of the upflow tubular reactor operating as a fixed bed (c) photograph of a foam coated with P25 catalyst.

Photocatalytic experiments were carried out in this reactor using three different TiO_2 based materials. Commercial Evonik P25 catalyst and two photocatalysts supplied by Tolsa S.A. named AQ-1 and Minclear WTT-P. The catalysts were used in both foams and suspensions and the catalyst load was optimized. The final values used in the photocatalytic experiments were 1 g/L for the suspensions and 1 g/foam when using supported catalyst.

The photocatalytic foams were prepared by (i) dipping a commercial ZrO_2 foam supplied by Insertec S.A into a photocatalyst suspension, and (ii) calcination at 500 °C for two hours. Each foam was 2.5 cm height, 3 cm inner diameter, 5 cm outer diameter and a porosity of 10 ppi (**figure S.4-c**). The photocatalyst loading on each foam was controlled by successive immersion cycles and calcination. For the photocatalytic experiments, six foams were located in the photoreactor being the total working height of 15 cm (**figure S.4-b**).

Summary

Photocatalytic experiments.

Bacterial inactivation.

Escherichia coli K12 strains (CECT 4624, corresponding to ATCC 23631, where CECT stands for "Colección Española de Cultivos Tipo") were used to prepare the bacterial suspensions (NaCl 0.9%). Fresh liquid cultures were prepared by inoculation in a Luria-Bertani (LB) nutrient medium (Miller's LB Broth, Scharlab) and incubation at 37 °C for 24 h under constant stirring on a rotary shaker. An initial bacterial concentration of 10^6 CFU mL⁻¹ was used in all the experiments. The analysis of the samples throughout the reaction was carried out following a standard serial dilution procedure. Each decimal dilution was spotted 4 times on LB nutrient agar plates and incubated at 37 °C for 24 h before counting. In order to test the reproducibility, all the experiments were performed at least twice being the results expressed as the mean and the experimental errors as the standard deviation.

Chemical oxidation.

Methanol (Sigma-Aldrich, LC-MS) was chosen as model chemical pollutant at initial concentration of 100 mM. All solutions were done in deionized water. The oxidation of methanol was followed through the colorimetric determination of the formaldehyde produced throughout the reaction, quantitative oxidation product when methanol is in excess¹⁷.

¹⁷ Cristina Pablos and others, 'Correlation between photoelectrochemical behaviour and photoelectrocatalytic activity and scaling-up of P25-TiO₂ electrodes', *Electrochimica Acta*, 130 (2014), 261–70.

Removal of CECs and simultaneous disinfection.

The removal of CECs and simultaneous disinfection was performed for both, synthetic water, and real wastewater treatment plant effluents from the secondary treatment of the Estiviel WWTP located in Toledo (Spain). In order to prepare the synthetic water *Escherichia coli* K12 strains with an initial concentration of 10^6 CFU/mL and a mix with 20 ppb of different CECs (**table S1**) were added to an aqueous solution of NaCl 0.9%.

Table S.1. Compounds in the mix of CECs added to the synthetic water.

Compound	Abbreviation	Compound	Abbreviation
4-Acetaminoantipyrine	4-AAA	Estrone	EST
Atenolol	ATN	Gemfibrozil	GFZ
Atrazine	ATZ	Hydrochlorothiazide	HCT
Azoxystrobin	AZX	Ibuprofen	IBP
Bisphenol A	BPA	Imidacloprid	IMD
Buprofezin	BPZ	Iohexol	IHX
Caffeine	CFN	Iopamidol	IPM
Carbamazepine	CBZ	Isoproturon	IPT
Clofibric Acid	CFA	Metamitron	MTM
Cyclophosphamide	CPD	Metoprolol	MTP
Diclofenac	DCF	Metronidazole	MDZ
Diethyltoluamide	DEET	Sulfamethoxazole	SMX
Dimethoate	DMT	Terbutryn	TBT

The analysis of the microorganism throughout the reaction was carried out following a process similar to the one explained above.

The CECs analysis was performed by LC-MS chromatography using a Varian 550-LC column valve module with a C18 column ($3\mu\text{M}$, 2.5×100 mm) after a C18 trap column. The mobile phases were: (A) 0.9% Glacial Acetic Acid in Milli-Q® ultrapure water and (B) 100% acetonitrile (flow

Summary

rate: 250 $\mu\text{L}/\text{min}$). A solid phase extraction using TELOS ENV cartridges, 6 cc, 200 mg and concentrated via elution with pure methanol was carried out previously. A Varian 325-MS triple quadrupole mass spectrometer with Varian MS Workstation 6.9.3 software was used for data collection and processing. Quantification was performed using an internal calibration curve prepared with standards at concentrations ranging from 1 to 50 $\mu\text{g}/\text{L}$. Deuterated or ^{13}C -labelled compounds were used to correct losses during the extraction process.

III. RESULTS AND DISCUSSION.

Optimization of light distribution on the photocatalytic reactor.

Light distribution calculations.

Figure S.5 shows the representation of the incident radiation, calculated with Ansys Fluent, along a longitudinal plane within the reaction area, for each lighting source, for the same total emission. It can be seen that there is a completely different distribution of the light in each case due to the different emitting surface of each lighting source. It can be seen how in the case of the Hg-FL a very homogeneous distribution of the light is achieved, however, in the case of the 8-LED system, there are areas with very high irradiation values corresponding to the areas where the LED are located, while other areas remain practically in darkness. On the other hand, the 40-LED system represents an intermediate case in which the homogeneity of the light distribution has been improved with the increase in the number of LEDs, but it has not been able to reach the level of homogeneity achieved with the Hg-FL.

The values of the uniformity index of the incident radiation for each of the lighting systems were calculated obtaining values of 0.685, 0.382 and 0.559 for Hg-FL, 8-LED and 40-LED respectively. These values confirm the best light distribution obtained when using Hg-FL previously observed in **figure S.5**, which can have important implications in the photonic efficiency of the reactor.

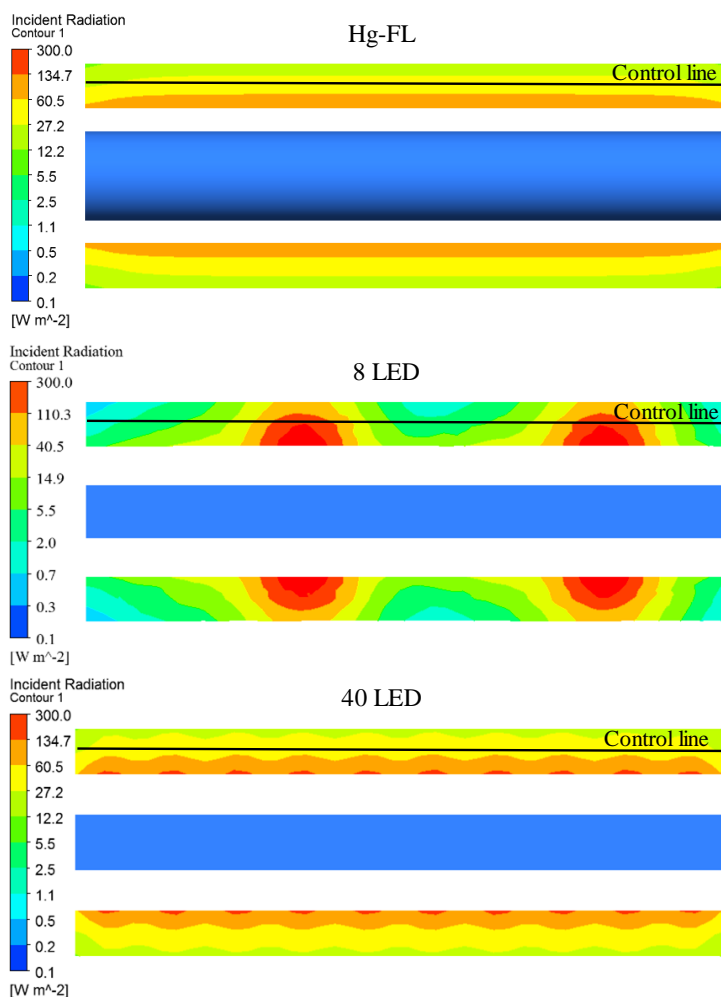


Figure S.5. Representation of the incident radiation along a longitudinal plane within the reaction area for the three lighting systems used.

Summary

Incident radiation and power consumption.

Actinometrical experiments for different emission conditions were carried out. **Figure S.6** shows the incident radiation values obtained in each case. It can be seen how, as expected, an increase in the electric intensity of the LED causes an increase in the amount of light emitted. However, this trend is not linear due to a lower efficiency of the LED systems when the electric intensity is increased. Thus, it is important to note that, for the same electrical energy consumption, the 40-LED system works with an electric intensity five times lower than the 8-LED system since it presents a number of LED five times higher.

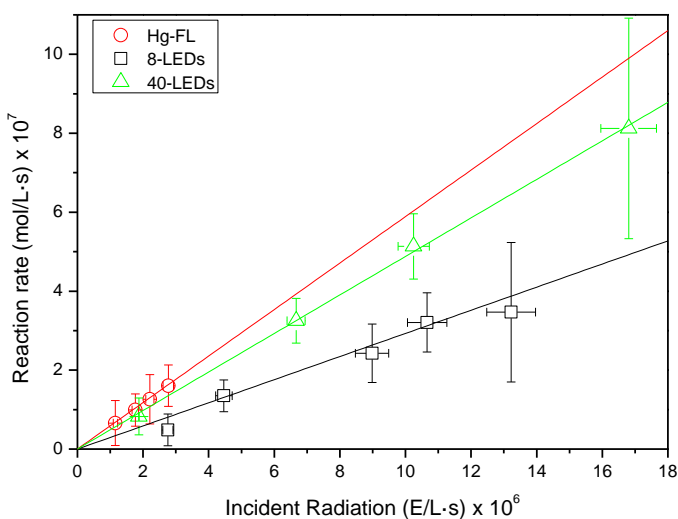


Figure S.6. Incident radiation versus power consumption for the three lighting sources.

If the efficiency of both systems is calculated in terms of photons produced per unit of energy consumed, averages values of 4.32 and 5.88 E kWh are obtained for the systems of 8 and 40 LEDs respectively, This results means

an improvement of 36% when using the 40 LED system. In the case of the Hg-FL, the value obtained when no attenuating filter is used is 1.4 E/kWh being as expected the worst efficient system.

Chemical oxidation

The methanol oxidation reaction rate when using P25 catalyst was calculated for different values of incident radiation with the three lighting systems. In all cases, it can be observed a linear dependence between the reaction rate and the incident radiation (**figure S.7-a**). Also, it can be seen how the values of the reaction rate for the Hg-FL lamp are much higher than for the LED systems when the same values of incident radiation are used. If the photonic efficiency is calculated as the moles of oxidized methanol per mole of incident photons (slopes of the lines in **figure S.7-a**) a value of 5.89 is obtained for the Hg-FL lamp, while in the case of the systems of 8 and 40 LEDs values of 2.9 and 4.9 are obtained respectively.

To explain these results, it is necessary to focus in the light distribution of each lighting system. Some studies observed that, when working with high incident radiation values, there is an increase in the electron-hole recombination phenomenon that produces a decrease in photocatalytic efficiency¹⁸. As was observed in **figure S.5** the light distribution when using Hg-Fl is very homogeneous not existing areas with high incident radiation values. The 8-LED system represents an opposite case because

¹⁸ Yash Boyjoo, Ming Ang, and Vishnu Pareek, 'CFD simulation of a pilot scale slurry photocatalytic reactor and design of multiple-lamp reactors', *Chemical Engineering Science*, 111 (2014), 266–77.

Cintia Casado and others, 'Comprehensive multiphysics modeling of photocatalytic processes by computational fluid dynamics based on intrinsic kinetic parameters determined in a differential photoreactor', *Chemical Engineering Journal*, 310 (2017), 368–80.

Summary

the emission of the same amount of light is carried out in 8 localized zones producing high incident radiation values in the adjacent areas. The 40-LED system is an improvement in this aspect because due to the increase in the LED number a more homogeneous distribution of light is achieved avoiding such a high recombination phenomenon. **Figure S.7-b** confirms the existence of a direct relationship between the uniformity index calculated for each system and its corresponding photonic efficiency, which will determine the overall efficiency of the process.

If the results are analysed in terms of energy consumption, it can be seen how the low energy efficiency of Hg-FL is counteracted by its better photonic efficiency compared to LED systems. The 8 LED system is capable to oxidize 0.166 moles of methanol per kWh consumed while the Hg-FL lamp oxidizes 0.11 moles per kWh. On the other hand, the 40 LED system is the most efficient lighting system oxidizing 0.367 moles of methanol per kWh. The greater energy efficiency of this system is due to both, an improvement in light distribution compared to the 8 LED system and an improvement in the conversion of electricity into light compared to the Hg-FL lamp.

These results show the critical role that the light distribution play in the efficiency of photocatalytic processes. Although the use of LED systems has been widely extended in the last years due to its greater energy efficiency, the results obtained confirm that, if a proper design of the reactor is not carried out, the overall efficiency of the process could not be improve with respect to the traditional use of mercury lamps.

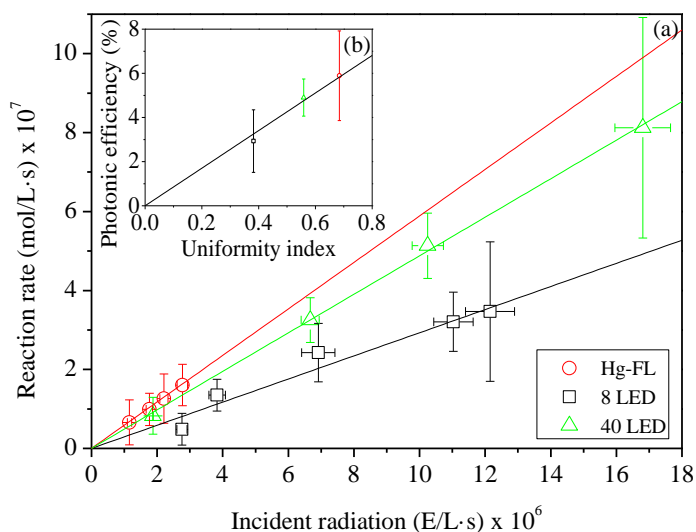


Figure S.7. (a) Methanol oxidation reaction rate for the different illumination sources versus incident radiation and (b) photonic efficiency versus uniformity index of each illumination source.

Bacterial inactivation.

Bacterial inactivation experiments were carried out under similar lighting conditions to those previously used in methanol oxidation. The inactivation profiles were adjusted using the mechanistic model developed by Marugán et al.¹⁹ and the kinetic constants were obtained. **Figure S.8** shows the inactivation rates obtained for each illumination source when different values of incident radiation are used. It can be seen as opposite what was observed for methanol oxidation, there is no clear differences in the inactivation rates with the different lighting systems.

¹⁹ Javier Marugán, Rafael van Grieken, and others, 'Kinetics of the photocatalytic disinfection of Escherichia coli suspensions', *Applied Catalysis B: Environmental*, 82.1 (2008), 27–36.

Summary

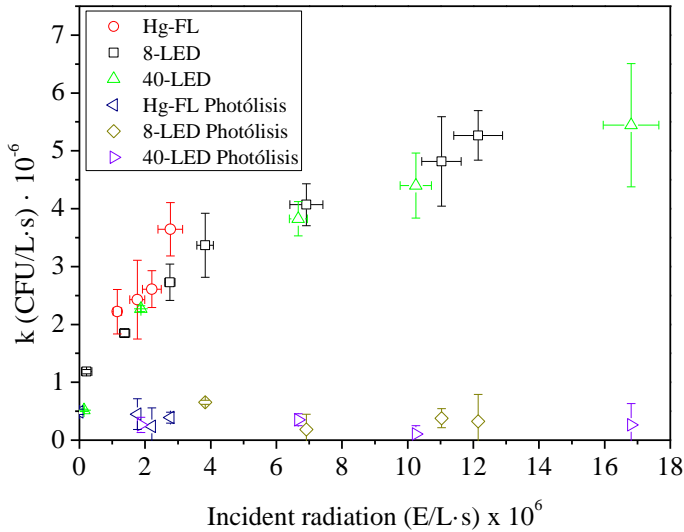


Figure S.8. *E. coli* inactivation rate versus the incident radiation for the different illumination sources.

These results are apparently in contradiction with the previous conclusions derived from the photocatalytic tests of methanol oxidation, where a more homogeneous distribution of the light implies a greater photonic efficiency. A possible explanation of this behaviour can be found in the works of Soomer et al.²⁰ and Pulgarin et al.²¹ where it was concluded that there are greater inactivation efficiencies when high UV intensities are applied due to a higher influence on the repairing enzymes of the cell.

According to this explanation, the results of **figure S.8** can be explained based on two opposite effects related to the light distribution. On the one

²⁰ R. Sommer and others, 'Time dose reciprocity in UV disinfection of water', *Water Science and Technology*, 38.12 (1998), 145–50.

²¹ A.G. Rincón and C. Pulgarin, 'Photocatalytic inactivation of *E. coli*: effect of (continuous–intermittent) light intensity and of (suspended–fixed) TiO₂ concentration', *Applied Catalysis B: Environmental*, 44.3 (2003), 263–84.

hand, for the pure photocatalytic process, there is an improvement in photonic efficiency when a more homogeneous distribution of light is achieved as was demonstrated in the methanol oxidation. However, on the other hand, this effect is counteracted by a greater inactivation of the bacteria when they are subjected to a high intensity of UV. This second effect, specific for the inactivation of microorganisms and not applicable to the oxidation of chemical products, makes the disinfection processes relatively independent of the distribution of the incident radiation.

In terms of energy consumption, because no clear differences in inactivation were observed when using the different lighting systems, the LED systems, and specifically the 40-LED system, are the most energy efficient systems due to their higher electrical efficiency.

Optimization of wavelength in photocatalytic and photo-Fenton processes.

Chemical oxidation.

In order to study the influence of the wavelength in the methanol oxidation, different 8 LED illumination sources with maximum emission peaks centered in wavelengths between 365 and 405 nm were used. Actinometrical reactions were carried out when using each illumination source obtaining values of electrical efficiency of 3.75, 4.87, 4.95, 5.54, 5.92 and 6.78 E/kWh for LED systems with maximum emission peaks centered in 365, 385, 390, 395, 400 and 405 nm respectively. In order to study the behaviour when using catalysts with different absorption

Summary

spectrum (**figure S.9**) experiments with both P25 and Fe-citrate catalysts were carried out.

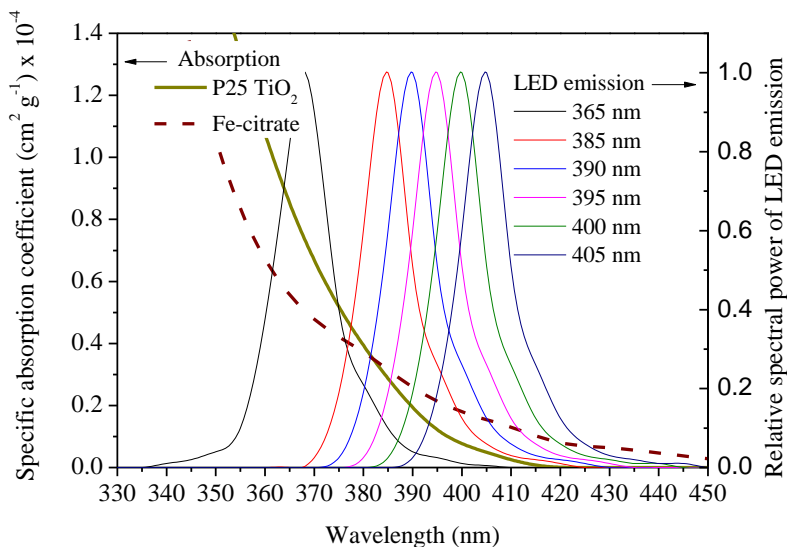


Figure S.9. Emission spectrum of the different LEDs and spectral distribution of the specific absorption coefficients for P25 and Fe-citrate catalysts.

When the P25 catalyst was used for the photocatalytic experiments, it could be observed how the highest reaction rate values were obtained for a wavelength of 365 nm. While, as the wavelength increases, a very pronounced decrease in the reaction rate occurs with negligible methanol oxidation at wavelengths higher than 390 nm. The behaviour of catalyst Fe-citrate is very different. Although, as with P25 catalyst, the maximum reaction rate was obtained for 365 nm, the increase in wavelength does not produce such a drop in the reaction rate, and a considerable methanol oxidation can be observed when the 405 nm LED system is used. This behaviour can easily be explained taking into account the absorption spectra of the two catalysts used. As seen in **figure S.9** for 365 nm, the P25 catalyst has a higher absorbance; however, as the wavelength is increased

this trend is reversed, with Fe-citrate catalyst having the highest absorption coefficient for wavelengths longer than 380 nm.

If the specific absorption coefficients are plotted together with the photonic efficiency as a function of the wavelength (**figure S.10**), it can be seen how in both cases the photonic efficiency obtained for each wavelength matches with the absorption spectrum of the catalyst. This is a very important aspect to take into account since it allows the estimation of the photonic efficiency for different wavelengths depending on the absorption spectrum without being necessary to carry out new experiments.

However, the most important aspect to consider when using artificial lighting sources is the energy consumption of the system. **Figure S.11** shows the energy efficiency as a function of wavelength. In it, it could be seen how in the case of the P25 catalyst due to the large drop in photonic efficiency when increasing the wavelength, the most recommended LEDs are clearly the 365 nm LED despite having a lower electrical efficiency. In the case of Fe-citrate catalyst, however, there is no such clear difference in energy efficiency between LEDs of different wavelengths. The worst photonic efficiency for LEDs with longer wavelengths is partially compensated by their better efficiency in the conversion of electricity to light.

Although experiments with lower wavelengths were not performed, it can be assumed that energy efficiency would not improve since there is a large drop in the electrical efficiency of LEDs emitting below 365 nm. On the other hand, no experiments were performed for higher wavelengths since the improvement in the electrical efficiency of the LEDs would no longer compensate the decrease in photonic efficiency.

Summary

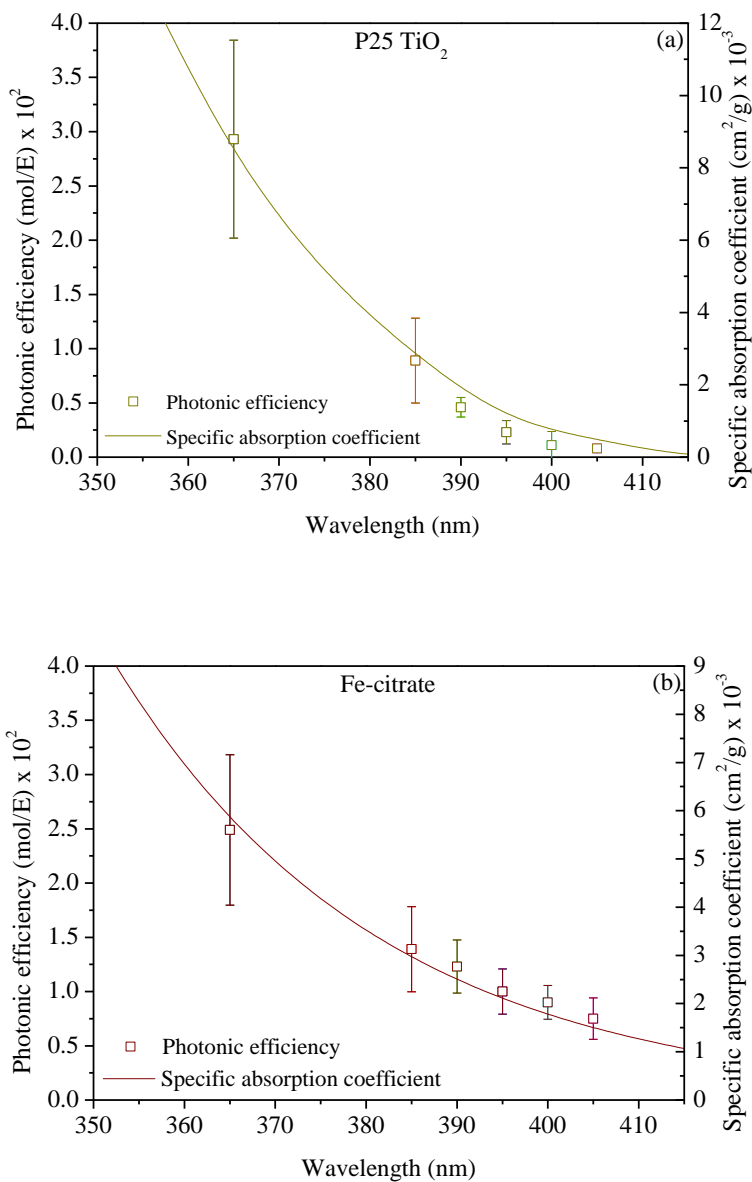


Figure S.10. Photonic efficiency of methanol oxidation and specific absorption coefficients versus wavelength for catalysts (a) P25 and (b) Fe-citrate.

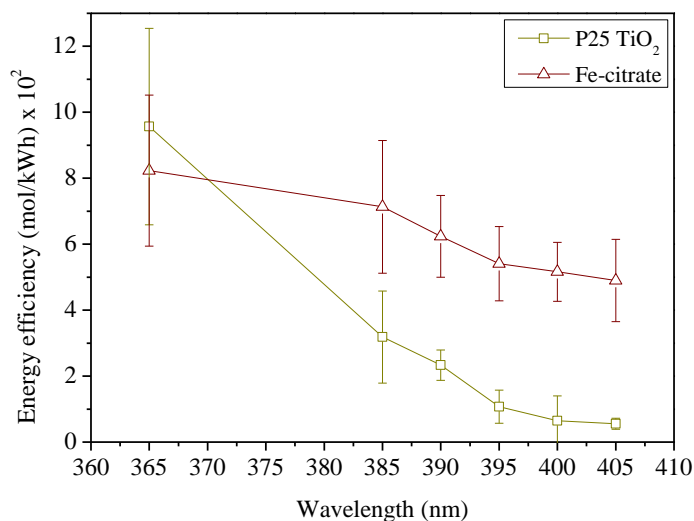


Figure S.11. Energy efficiency of methanol oxidation versus wavelength for P25 and Fe-citrate catalysts.

Influence of wavelength in bacterial inactivation.

To investigate the existence of possible differences between bacterial inactivation and methanol oxidation, bacterial inactivation experiments were carried out for wavelengths of 365, 385 and 405 nm. The kinetic constants were obtained again by adjustment with the mechanistic model developed by Marugán et al.²². It could be observed that, as happened with the methanol oxidation when using P25 catalyst, there is a great difference between the different wavelengths used, existing a very pronounced drop in the inactivation rate when increasing the wavelength. On the contrary, in the case of Fe-citrate catalyst this difference between wavelengths is not so clear.

²² Marugán, van Grieken, and others. Kinetics of the photocatalytic disinfection of Escherichia coli suspensions, Appl. Catal. B Environ. 82 (2008) 27–36.

Summary

Again, to find the explanation for this behaviour, it is necessary to look at the absorption spectra of the catalysts. In **figure S.12**, it can be seen that just as for the oxidation of methanol, the inactivation efficiency of bacteria matches with the absorption spectra of the catalysts.

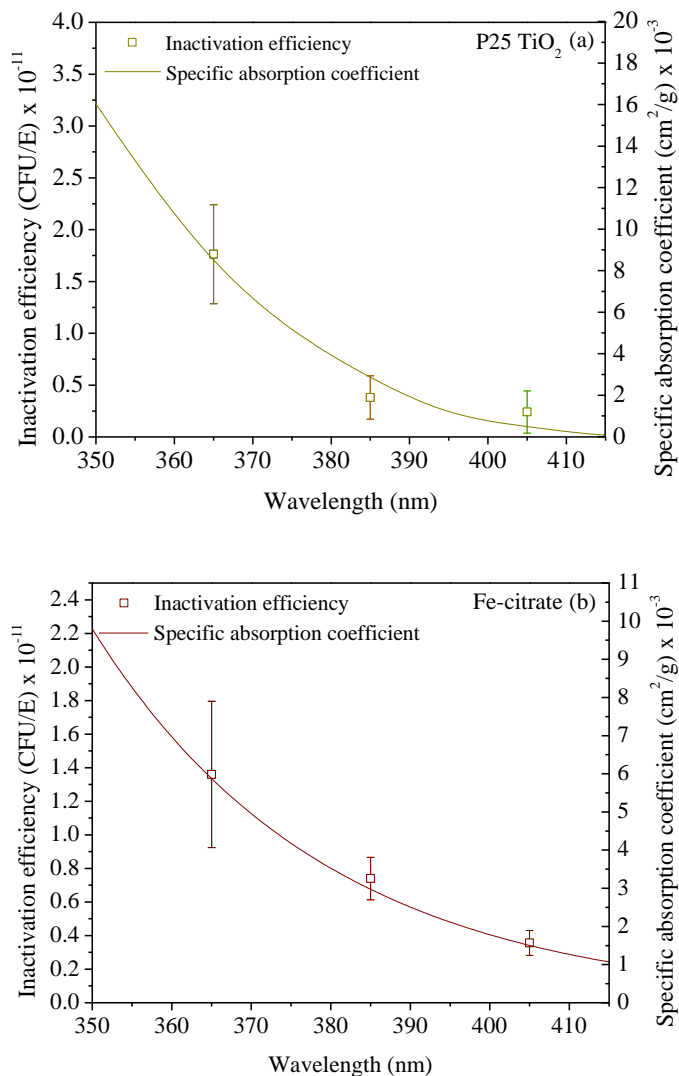


Figure S.12. Efficiency of bacterial inactivation and specific absorption coefficients versus wavelength for catalysts (a) P25 and (b) Fe-citrate.

These results show that the only step dependent on the wavelength in the interval studied in both bacterial inactivation and chemical oxidation is the generation of electron-hole pairs, while the remaining steps depend only on the oxidative capacity of the hydroxyl radicals generated.

In terms of energy efficiency in **figure S.13**, it can be seen how the results are similar with those obtained for methanol oxidation. For the selected catalyst concentrations, the highest energy efficiency is obtained for a wavelength of 365 nm when P25 catalyst is used. However, when LEDs with longer wavelengths are used, the use of Fe-citrate as a catalyst is more cost-effective.

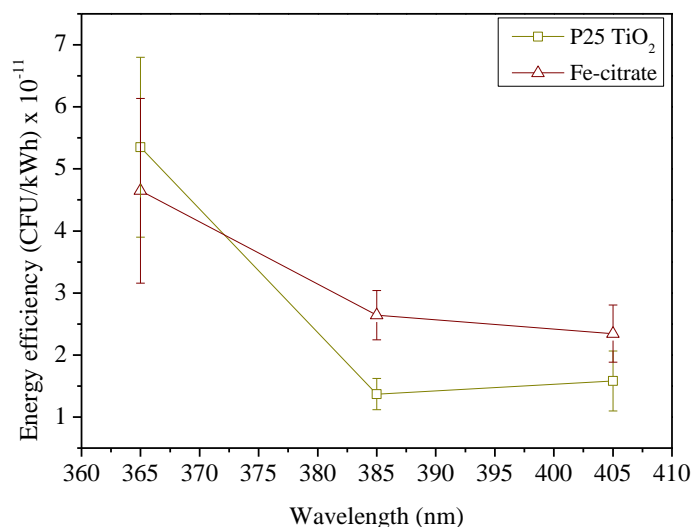


Figure S.13. Energy efficiency of bacterial inactivation versus wavelength for P25 and Fe-citrate catalysts.

Solar irradiation.

As previously mentioned, a particularly interesting option for the application of photocatalytic processes is the use of solar light. In this

Summary

section, a predictive estimation of the activity of the two catalysts studied was carried out if the Sun is used as illumination source. Due to the polychromatic nature of sunlight, it was necessary to carried out a discretization estimating the photonic efficiency that would be obtained for each individual wavelength and subsequently calculating the overall efficiency by integrating the efficiency of the process for each specific wavelength.

The photonic efficiency (mol/E) for each individual wavelength in the 365-405 nm range was calculated by interpolation of the results shown in **figures S.10** for methanol oxidation and **figure S.12** for bacterial inactivation. To define the solar irradiation, the solar spectrum AM 1.5 based on the ASTM G173-03 standard was taken as a reference since it is the spectrum most commonly used in the industry. Taking into account these data, the methanol that would be oxidized and the bacteria that would be inactivated for each wavelength was calculated and are shown in **figure S.14**. If the integral of each reaction rate function is performed, an estimation of the overall reaction rate for the studied range of wavelengths can be obtained for each case. Values of 1.27×10^{-8} and 1.92×10^{-8} mol/L·s were obtained for the methanol oxidation with P25 catalyst and Fe-citrate catalyst respectively. In the case of bacterial inactivation values of 7.38×10^4 and 1×10^5 CFU/L·s were obtained for P25 catalyst and Fe-citrate catalyst respectively. This means that when Fe-citrate catalyst is used under UV-A solar irradiation, the expected activity is 50% and 35% higher for methanol oxidation and bacterial inactivation respectively than when P25 catalyst is used. Both the results of bacterial inactivation and chemical oxidation show improvement with the use of Fe-citrate catalyst with sunlight compared to the traditional use of P25 catalyst, which makes it a

very attractive alternative to improve the efficiency of photocatalytic processes when using sunlight.

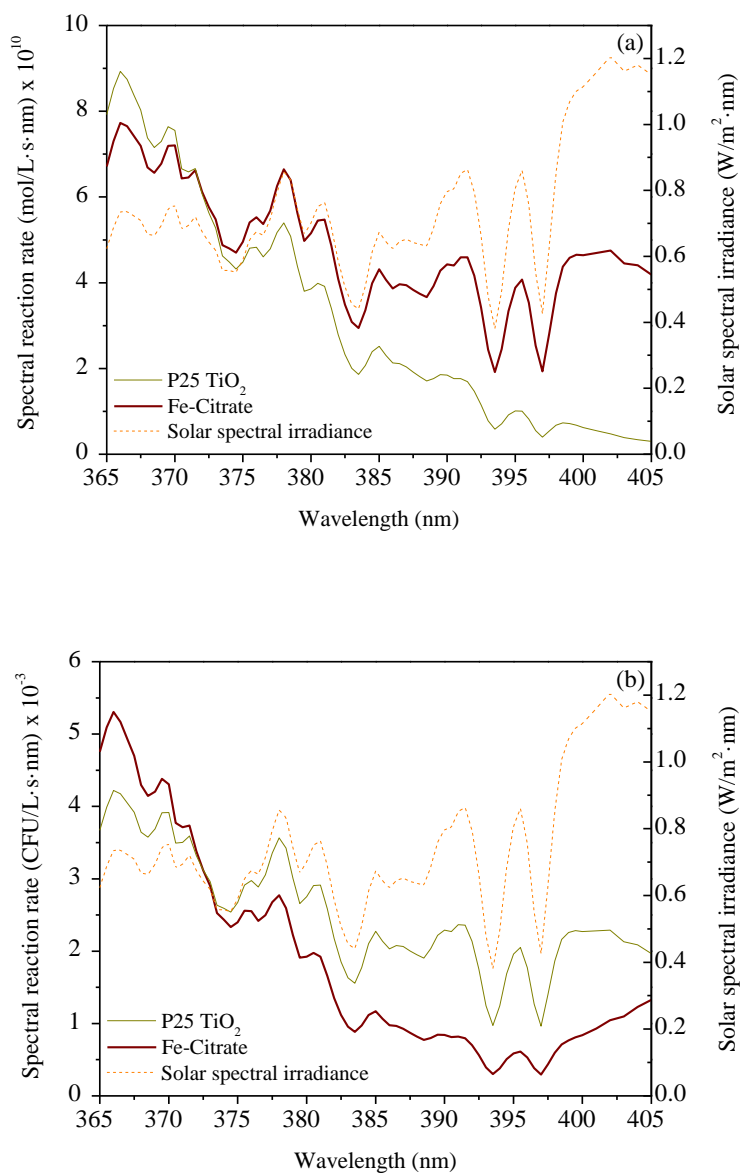


Figure S.14. Spectral reaction rate calculated as a function of the solar spectrum for P25 and Fe-citrate catalysts for (a) methanol oxidation and (b) bacterial inactivation.

Summary

It must be borne in mind that, although this study has been carried out in a small range of wavelengths and the results must be treated with care. It is considered that these correctly represent the general behaviour of the two catalysts since at higher wavelengths than those studied, there is a very low absorption for both catalysts while in wavelengths below 365 nm there is a very low solar radiation.

In order to validate these predictions, experiments of methanol oxidation and bacterial inactivation were carried out in a CPC reactor under sunlight on different days of June 2017 at the facilities of the Rey Juan Carlos University in Móstoles, Spain (40.33 °N, 3.88 °W). The reaction rates in each case were calculated taking into account the solar irradiation accumulated during the experiments. In **figure S.15**, the average reaction rate value can be seen for both P25 and Fe-citrate catalysts. The results show improvements of 38% and 39% for methanol oxidation and bacterial inactivation, respectively, when Fe-Citrate catalyst is used with respect to the use of P25 catalyst. These results confirm the estimated improvement that was previously calculated when Fe-citrate catalyst is used. The differences between the values of the relative improvement of the experimental data and those predicted according to the action spectra may be due to the limitation of not using the complete solar spectrum and the possible experimental errors. These results confirm a significant improvement when using Fe-citrate catalyst over the traditional use of P25 catalyst offering the interesting possibility of using photo-Fenton reactions at neutral pH with Fe-citrate catalyst for the treatment of water when working under solar irradiation.

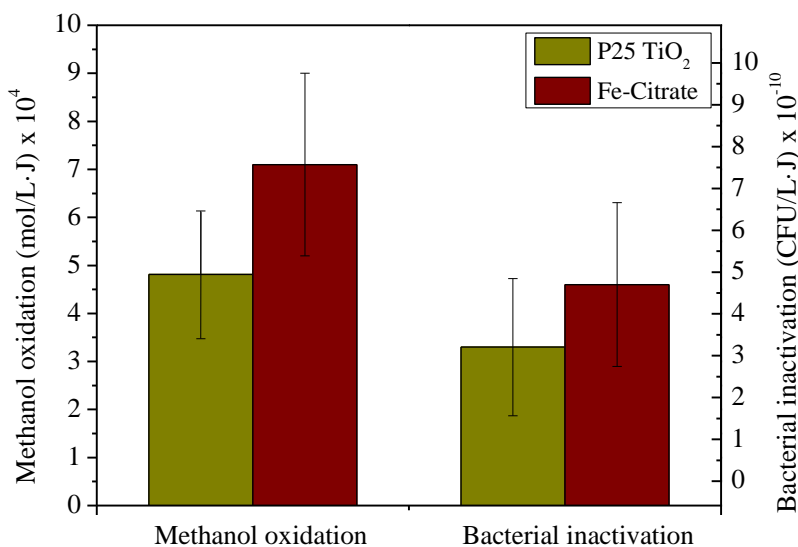


Figure S.15. Reaction rate of methanol oxidation and bacterial inactivation under sunlight in the CPC reactor.

Optimization of catalyst loading and reactor configuration

Three different materials based on TiO₂ (P25, WTT-P and AQ-1) were used to treat both synthetic water and real wastewater. The amount of each catalyst deposited in the foams was optimized by performing methanol oxidation reactions with foams with different catalyst loads. It was observed that for the three catalysts an increase in the catalyst load causes an increase in the photocatalytic oxidation rate of methanol until reaching a maximum value. An increase in the catalyst load above 1 g/foam does not lead to an increase in the kinetic constant in any of the catalysts so it was chosen as the optimum load to be used in the subsequent photocatalytic experiments. In order to verify the stability of the foams, 10 consecutive methanol reactions were carried out with the different foams confirming the results that there was no loss of activity for any of the three catalysts.

Summary

On the other hand, the optimization of the catalyst concentration in suspensions was also carried out using methanol oxidation as a test reaction. For the catalysts AQ-1 and WTT-P an optimum concentration of 1 g/L was obtained while for the P25 catalyst an optimum concentration of 0.1 g/L was obtained due to its better optical properties. In all cases, the concentration chosen for the subsequent experiments was 1 g/L. In the case of P25 catalyst, although the optimum concentration was reached for 0.1 g/L, a working concentration of 1 g/L was also chosen for comparative purposes, further ensuring that this concentration value also guarantees maximum removal efficiency. For all subsequent experiments with both foams and suspensions, an electricity current of 100 mA was set in the lighting source.

It is important to note that when comparing the methanol oxidation reaction rates obtained for both foams and suspensions, its observed how the maximum values obtained are similar regardless of whether the catalyst is supported or not. The high concentration of methanol and the structure of the foams seem to prevent the reaction rate from being limited by the transfer of matter.

Treatment of synthetic water.

The treatment of a synthetic water was carried out with both the foams and the suspensions. The results obtained for the elimination of the CECs were adjusted to a first-order kinetics as previously described by other researchers²³ and the efficiencies of elimination of each compound are

²³ N. Miranda-García and others, 'Degradation study of 15 emerging contaminants at low concentration by immobilized TiO₂ in a pilot plant', *Catalysis Today*, 151.1–2 (2010), 107–13.

shown in **figure S.16**. It can be seen how some of the compounds are lightly removed by photolysis. However, to achieve higher elimination rates, it is necessary to incorporate the use of catalysts into the process. In the case of suspended catalysts, it can be observed how the treatment is very effective for a large number of compounds and most of the compounds can be eliminated at least 95% in 1 hour of treatment. However, some of them (ACFK, ATZ, CPD, DEET, IHX, IMD, IPM, MDZ) are more recalcitrant to the treatment and required at least 4 hours to achieve a 95% elimination. On the other hand, when the foams are used, it can be observed that for any of the compounds it is possible to achieve eliminations above 95% before 1.5 hours being necessary reaction times of more than 4 hours for most of them.

Additionally, it is possible to observe how the elimination efficiencies are similar for the three catalysts used in both foams and suspensions. However, it is observed that contrary to what happened in the case of methanol oxidation there are significant differences between the use of suspended catalysts and foams. In this case, the low concentration of CECs gives rise to diffusive problems that limit the effectiveness of the supported catalyst.

Summary

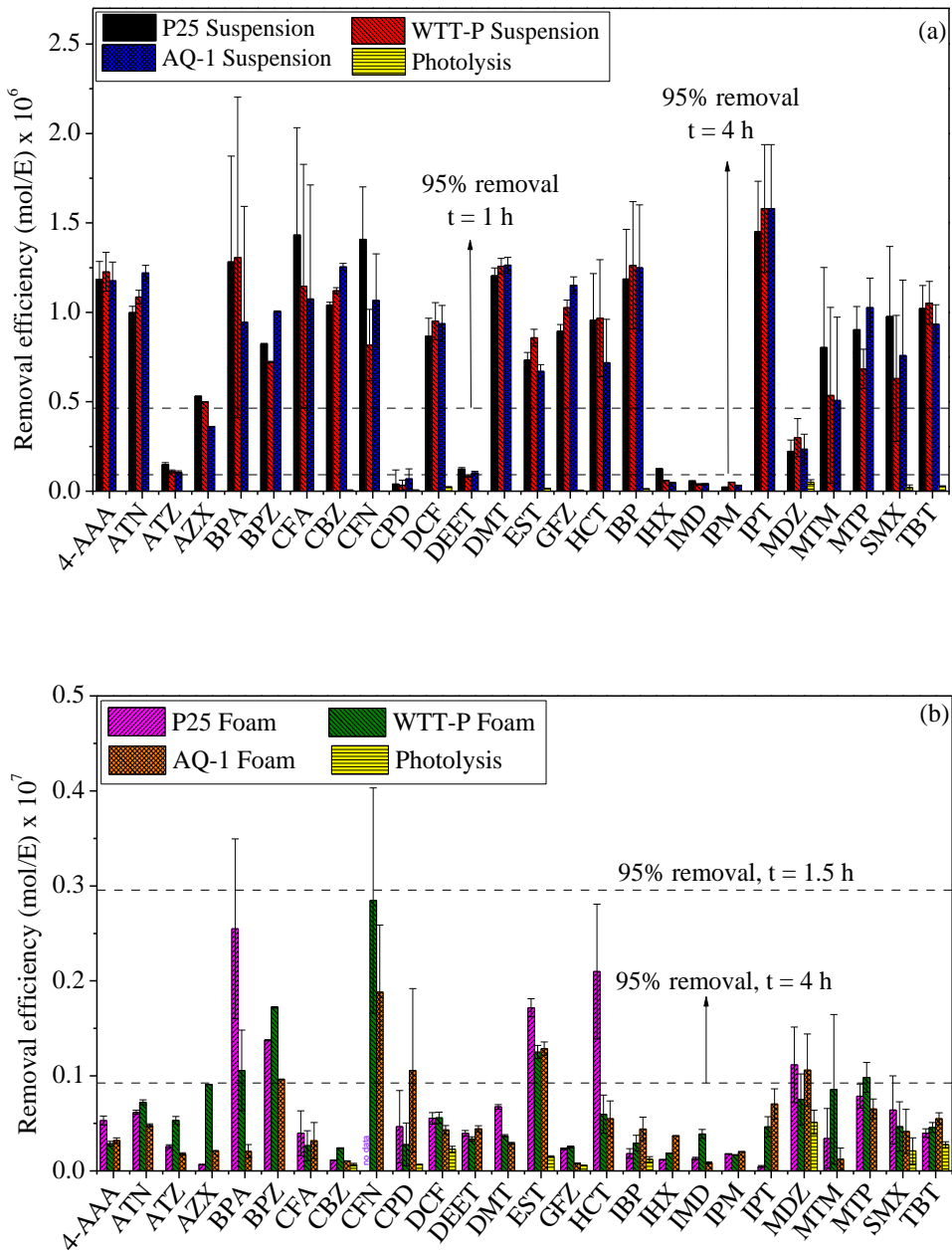


Figure S.16. Efficiencies of elimination of CECs in the treatment of synthetic water when catalysts are used in (a) suspensions and (b) supported in foams.

Regarding the bacterial inactivation, in **figure S.17** the profiles of viable *E. coli* obtained throughout the different reactions can be seen. It can be observed how there is a reduction in the concentration of viable bacteria colonies throughout the reaction, which indicates that it is possible to carry out simultaneously the elimination of CECs and bacterial inactivation due to the non-selectivity of the hydroxyl radicals. On the other hand, it can be seen that as in the treatment of CECs, the inactivation obtained when using the foams are lower than when the suspended catalyst is used due to diffusive problems.

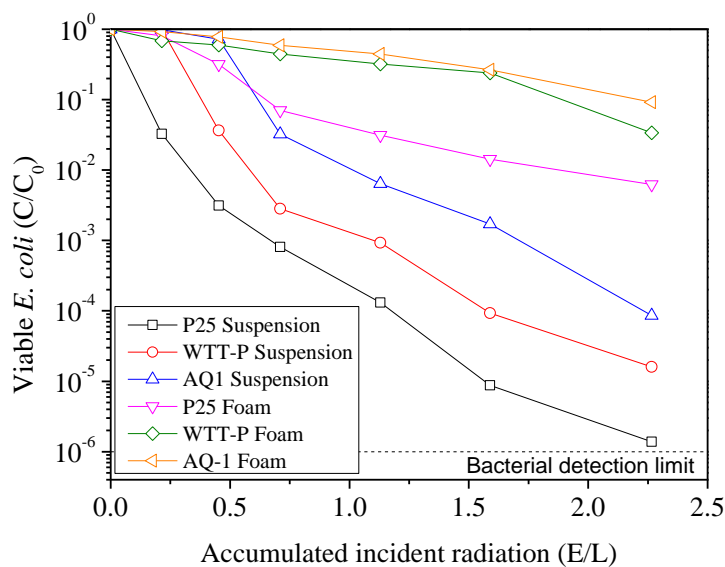


Figure S.17. Concentration of viable *E. coli* during the disinfection process of synthetic water with the different catalytic systems.

Treatment of EDAR effluents.

Photocatalytic experiments with WWTP effluents were carried out under the same conditions as those used in the experiments with synthetic water.

Summary

The initial concentration of CEC detected in the effluents of the WWTP are shown in **table S2**.

Table S.2. Initial concentration of CECs in WWTP effluents.

Compound	Concentration (ppb)
4-AAA	0.277 ± 0.027
ATN	0.164 ± 0.05
CBZ	0.584 ± 0.053
DCF	0.623 ± 0.057
GFZ	0.094 ± 0.037
HCT	0.56 ± 0.09
MTP	0.037 ± 0.009
TBT	0.217 ± 0.027

In **figure S.18**, it can be seen how again the elimination efficiencies of the three catalysts used are similar. In addition, it can be seen that as in the case of methanol oxidation and contrary to what happened in the synthetic water treatment, there are no significant differences between the use of the supported and suspended catalyst.

To explain this behaviour, it is necessary to focus on the limiting stage in each case. In methanol oxidation reactions, the high concentration of methanol avoids the existence of diffusive problems, being the limiting stage in this case the oxidation reaction of methanol that is limited by the availability of hydroxyl radicals. In the case of the treatment of synthetic water, however, the concentration of pollutants is very low, being the ratio of hydroxyl radicals/pollutants very high. In this case, the limiting stage is the diffusion of the pollutants. Taking this into account, the effectiveness

of the supported catalyst in the foams is clearly impaired with respect to the use of suspensions, obtaining lower elimination efficiencies.

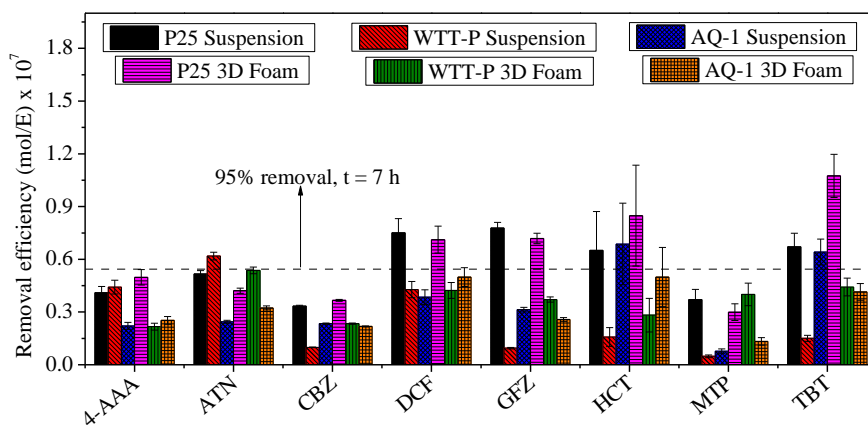


Figure S.18. Efficiencies of elimination of CECs when the different catalysts are used both in suspension and foams in the treatment of EDAR effluents.

In the treatment of EDAR effluents, due to the non-selectivity of the hydroxyl radicals, an important part of them are consumed in the oxidation of other organic compounds without interest present in the effluents. Therefore, despite the low concentration of CECs in water, the limiting step is not the diffusion but the availability of hydroxyl radicals to attack the molecules of interest. Therefore, no differences are observed in terms of photocatalytic activity between the use of the catalyst in suspension or supported in the foams.

Since, as previously explained in the treatment of EDAR effluents, there are limitations in the production of hydroxyl radicals, it can be explained that the efficiencies of elimination of CECs obtained are lower than those obtained for synthetic water, requiring at least 7 hours to reach 95% eliminations in most of the CECs. The elimination efficiency of these

Summary

compounds could be increased if the production of hydroxyl radicals is increased.

In the same way, in **figure S.19**, it can be observed how in the disinfection process there are no significant differences between the use of foams and suspended catalysts.

Taking into account all the above, it can be concluded that in the treatment of EDAR effluents both, the elimination of CECs and disinfection, are limited exclusively by the availability of hydroxyl radicals being the use of photocatalytic foams a good option for its treatment that avoids the necessity of a separation stage and makes the reuse possible.

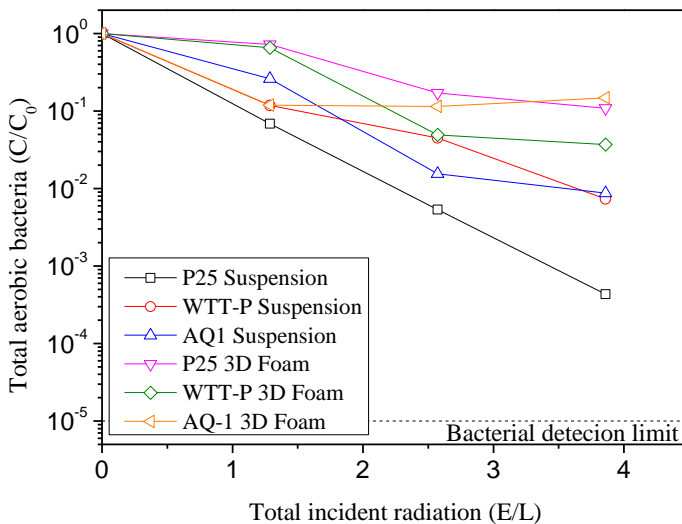


Figure S.19. Concentration of total aerobic bacteria throughout the treatment of EDAR effluents.

IV. CONCLUSIONS.

As could be verified throughout this work, LED-based lighting devices are more efficient in the conversion of electricity into light than traditional mercury lamps; however, their use can lead to non-homogeneous light distribution inside the reactor that can affect the photocatalytic efficiency. The photocatalytic methanol oxidation experiments allowed concluding that an improvement in the distribution of light produces a significant increase in the global photonic efficiency of the reactor. On the contrary, in bacterial inactivation, this higher photonic efficiency is counteracted by a greater bacterial inactivation when subjected to locally high UV intensities.

Both in the oxidation of chemical pollutants and in bacterial inactivation, it was concluded that the best option in terms of energy consumption is the use of lighting systems with a greater number of LEDs due to the improvement in electrical efficiency and in the homogeneity of the light distribution.

On the other hand, in the study of the influence of wavelength in the photocatalytic efficiency, it was possible to conclude the existence of a direct relationship both for chemical oxidation and for bacterial inactivation between photonic efficiency and the absorption spectrum of the catalyst used. The maximum energy efficiency when the P25 catalyst is used is reached for a wavelength of 365 nm resulting in an increase of it in completely inefficient processes. In the case of Fe-citrate catalyst, a very different behaviour has been observed since the photonic efficiency does not decrease so sharply with the increase in wavelength. This fact, together with the improvement of electrical efficiency for longer wavelengths, makes economically feasible to use wavelengths close to visible for both bacterial inactivation and chemical oxidation. In addition, the predictions

Summary

made for solar irradiation conditions based on the action spectra of the catalysts were successfully validated experimentally, demonstrating that the use of Fe-citrate catalyst represents significant improvements when working with solar light as a source of illumination.

Regarding the study of the use of supported catalysts, it was concluded that in spite of the fact that in the treatment of synthetic water the use of the supported catalyst in foams showed lower kinetic constants, this does not happen in the treatment of EDAR effluents. This fact shows that the use of this type of supports is as effective as the processes with the catalyst in suspension, offering the advantage of avoiding a subsequent separation stage and enables its reuse.

It was also demonstrated how it is possible to simultaneously carry out the elimination of CECs and bacterial inactivation, making possible its use as an additional tertiary treatment for wastewater treatment plants thus avoiding their discharge into the environment. It is also important to bear in mind that the catalysts AQ-1 and WTT-P achieved maximum elimination efficiencies similar to those achieved by the P25 catalyst, so they can be considered an effective alternative to the traditional use of commercial P25 catalyst.